JACS
JOURNAL OF THE AMERICAN CHEMICAL SOCIETY
Article
pubs.acs.org/JACS

Mechanistic Insights into the 1,3-Xylanases: Useful Enzymes for Manipulation of Algal Biomass

Ethan D. Goddard-Borger,[†] Keishi Sakaguchi,[‡] Stephan Reitinger,[†,∥] Nobuhisa Watanabe,[§] Makoto Ito,[‡] and Stephen G. Withers*[,†]

[†]Department of Chemistry, University of British Columbia, 2036 Main Mall, Vancouver, British Columbia V6T 1Z1, Canada

[‡]Department of Bioscience and Biotechnology, Graduate School of Bioresource and Bioenvironmental Sciences, Kyushu University, Fukuoka 812-8581, Japan

[§]Department of Biotechnology, Graduate School of Engineering, Nagoya University, Nagoya 464-8603, Japan

Supporting Information

ABSTRACT: Xylanases capable of degrading the crystalline microfibrils of 1,3-xylan that reinforce the cell walls of some red and siphonous green algae have not been well studied, yet they could prove to be of great utility in algaculture for the production of food and renewable chemical feedstocks. To gain a better mechanistic understanding of these enzymes, a suite of reagents was synthesized and evaluated as substrates and inhibitors of an *endo*-1,3-xylanase. With these reagents, a retaining mechanism was confirmed for the xylanase, its catalytic nucleophile identified, and the existence of −3 to +2 substrate-binding subsites demonstrated. Protein crystal X-ray diffraction methods provided a high resolution structure of a trapped covalent glycosyl−enzyme intermediate, indicating that the 1,3-xylanases likely utilize the $^{1}S_{3} \rightarrow {}^{4}H_{3} \rightarrow {}^{4}C_{1}$ conformational itinerary to effect catalysis.

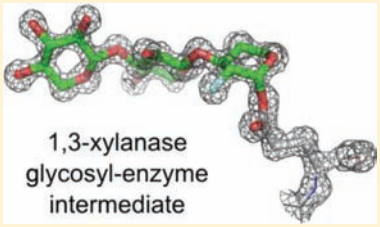

INTRODUCTION

Collectively, the algae produce a considerable number of unusual polysaccharides that are not found in higher plants. This is perhaps a consequence of their broad taxonomic diversity, simple body plan, and the unique challenges and opportunities presented by their aquatic environments. The composition of algal cell walls can vary radically between phyla, in contrast to the higher plants, which for the most part utilize a common system of cell wall polysaccharides and are invariably reliant on cellulose for cell wall strength. A number of algae produce cell walls that are completely devoid of cellulose, a curious observation first noted over a century ago[1] and unequivocally confirmed some six decades later.[2] Many of these cellulose-free algae rely on other polysaccharides to endow their cell walls with the mechanical properties necessary to survive. One such polymer is 1,3-xylan, a homopolysaccharide of β-1,3-linked D-xylopyranose units, which is found in some red and siphonous green algae. Within these organisms, molecules of 1,3-xylan bundle into right-handed triple helices, which pack hexagonally to form crystalline microfibrils.[3,4] These fibrils envelope the algal cell in transverse, longitudinal, and/or random orientations, just as cellulose microfibrils do in higher plants.[5]

A number of algae possessing 1,3-xylan-based cell walls are of significant relevance to human activities. Many red algae cultivated for human consumption, such as those harvested as Japanese "nori", Korean "gim", Anglo-American "dulse", and "laver", are *Porphyra* species that possess cell walls reinforced by microfibrils of 1,3-xylan.[6] Of the many siphonous green algae that produce 1,3-xylan, two *Caulerpa* species are of particular note: *Caulerpa lentillifera* (cultivated for human consumption)[7] and *Caulerpa taxifolia* (a highly invasive pest).[8]

Understanding how Nature goes about depolymerizing 1,3-xylan goes beyond a general interest in the ecology of these algae. Enzymes capable of degrading 1,3-xylan are currently used to degrade the cell wall of living algal cells in order to generate protoplasts, which enables cell fusion and genetic manipulation to create new cultivars with characteristics that are desirable for algaculture.[9] It has also been suggested that 1,3-xylan-containing algal biomass could serve as a feedstock for the production of renewable chemical commodities.[10] If such technology were developed, the 1,3-xylanases (EC 3.2.1.32) would no doubt play a central role in the conversion of that biomass into useful products.

Enzymes capable of degrading 1,3-xylan were first alluded to by Iriki and co-workers in the 1960s, when it was noted that several fungal species appeared to secrete enzymes capable of hydrolyzing the 1,3-xylan that they had only recently isolated from siphonous green algae.[11] Some time later, several fungal proteins with 1,3-xylanase activity were isolated from the culture medium of an *Aspergillus terreus* strain that originated from soil collected near a seaweed-processing factory.[12] Since then a number of secreted 1,3-xylanases induced by the presence of 1,3-xylan have been identified in bacteria cultured from marine sediments.[13−15] The genes encoding several of these bacterial 1,3-xylanases (from various *Alcaligenes*, *Vibrio*, and *Pseudomonas* species) have since been cloned and

Received: December 19, 2011
Published: January 30, 2012

   dx.doi.org/10.1021/ja211836t | *J. Am. Chem. Soc.* 2012, 134, 3895−3902

recombinantly expressed in *E. coli*, and to date, they are the only functionally characterized 1,3-xylanase genes.[16−18]

Bacterial 1,3-xylanases, like many cellulases, hemicellulases, and chitinases, have a modular architecture: they consist of a catalytic domain, glycine rich linker(s), and one or more carbohydrate binding modules (CBMs).[17,18] The unique CBMs of the 1,3-xylanases belong to CBM family 31 of the Carbohydrate Active enZyme (CAZy) database (http://www.cazy.org),[19] and they are characterized by an immunoglobulin-like fold with high affinity only for insoluble, crystalline 1,3-xylan microfibrils.[18,20,21]

The catalytic modules of the known 1,3-xylanases all belong to glycoside hydrolase (GH) family 26 of the CAZy database. This sequence-based classification suggests that these xylanases are retaining GHs, although this detail has yet to be empirically confirmed for this subclass of enzymes. GH family 26 also harbors β-mannanases (EC 3.2.1.78)[22] and lichenases (EC 3.2.1.73).[23] These two enzymes act on very different substrates and invoke different pyranose conformational itineraries for the electrophilic migration events that occur during catalysis.[24] The mannanases appear to operate with a $^{1}S_{5} \rightarrow B_{2,5} \rightarrow {}^{O}S_{2}$ itinerary,[25] while the lichenases utilize a $^{1}S_{3} \rightarrow {}^{4}H_{3} \rightarrow {}^{4}C_{1}$ mechanism.[26] The conformational itinerary of the 1,3-xylanases remains unknown, although, based on studies of the 1,4-xylanases, only two possibilities are likely: the $^{1}S_{3} \rightarrow {}^{4}H_{3} \rightarrow {}^{4}C_{1}$ and $^{5}S_{1} \rightarrow {}^{2,5}B \rightarrow {}^{2}S_{O}$ itineraries.[24]

From the extensive body of literature describing the 1,4-xylanases, it is evident that the development of a range of unnatural substrates and inhibitors has been invaluable in delineating the details of the 1,4-xylanase mechanism.[27−32] Similar molecular tools are required to foster more detailed investigations of 1,3-xylanases; to date, no inhibitors or chromogenic/fluorogenic substrates have been described for these enzymes. The present work describes the development and evaluation of such compounds, as well as their use in addressing some of the mechanistic questions that remain unanswered for the 1,3-xylanases.

RESULTS AND DISCUSSION

Substrates. A number of fluorogenic oligosaccharide substrates were initially synthesized to simplify the kinetic analysis of 1,3-xylanases and to provide some insight into their substrate preferences, which would then inform the design of inhibitors. 1,3-Xylan is not currently commercially available, which means that the preparation of 1,3-linked *xylo*-oligosaccharides from natural sources is somewhat impractical. As a consequence, the substrates were instead assembled from monosaccharide synthons.

The known trichloroacetimidate **1**[33] and alcohol **2**[34] were prepared from D-xylose and used to synthesize the β-1,3-linked disaccharide **3** (Scheme 1). This product was treated with hydrogen bromide in acetic acid, presumably providing the corresponding glycosyl bromide, which was used to perform a Koenigs−Knorr glycosidation of 4-(trifluoromethyl)-umbelliferone (CF_3UB) to return disaccharide **4**. This product was subjected to a Zemplén transesterification to provide the desired disaccharide **5**.

Some polysaccharide-processing GHs are capable of performing transglycosylation at comparable rates to hydrolysis, which complicates kinetic characterization. In this event, substrates that cannot act as glycosyl acceptors can be very useful for studying the kinetics of hydrolysis.[35] For this reason, a similar sequence of reactions was used to synthesize the 3′-*O*-methyl

Scheme 1. Synthesis of Disaccharide Substrates 5 and 6

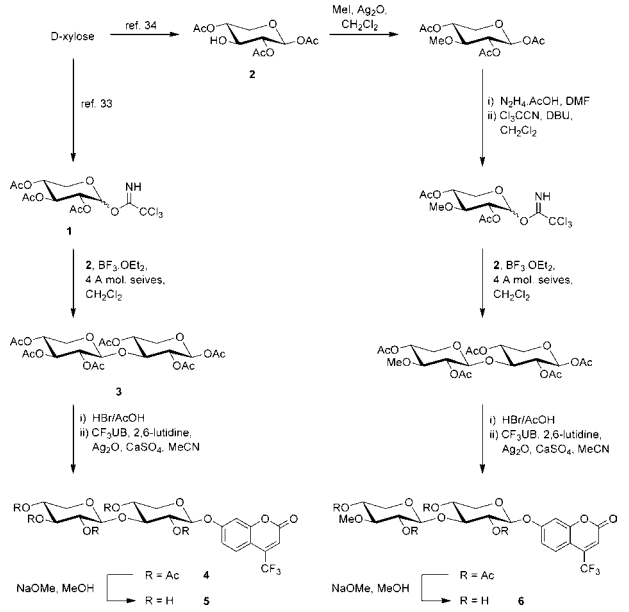

disaccharide **6**, which would likely be a poor glycosyl acceptor for 1,3-xylanases and thus minimize any potential competitive transglycosylation reactions.

Many endo-acting GHs prefer or require oligosaccharide rather than disaccharide substrates, although kinetic analyses can sometimes be complicated by the hydrolysis of several different glycosidic bonds within the substrate. Regardless, such substrates can be useful for exploring the role of more distant substrate binding subsites in catalysis. A [2 + 1] glycosylation strategy was employed to assemble the β-1,3;β-1,3-linked trisaccharide **7**. To prepare a suitable acceptor, triacetate **2** was chloroacetylated at O-3 and then converted into the known glycosyl bromide **8** (Scheme 2). Koenigs−Knorr glycosidation

Scheme 2. Synthesis of Trisaccharide Substrate 7

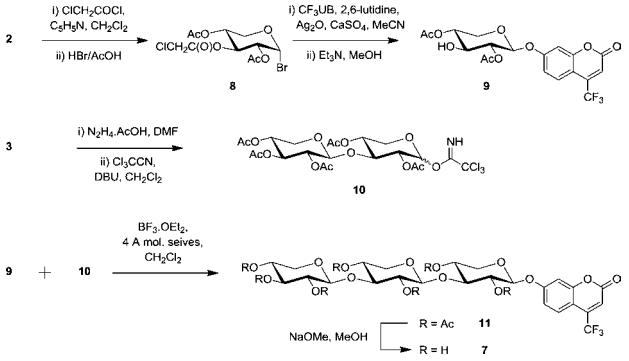

of 4-(trifluoromethyl)umbelliferone and base-catalyzed transesterification of the chloroacetate ester provided alcohol **9**. The β-1,3-linked disaccharide **3** was converted into the trichloroacetimidate **10** and then used to glycosylate alcohol **9**, providing trisaccharide **11** in good yield. As before, a base-catalyzed transesterification was used to effect deacetylation, providing the desired product **7**.

The glycosides **5**−**7** were evaluated as substrates for Xyl4, the *endo*-1,3-xylanase from *Vibrio* sp. strain AX-4 (Table 1).[17] The enzyme was capable of processing both disaccharide substrates **5** and **6**, but it exhibited markedly greater activity on the

dx.doi.org/10.1021/ja211836t | J. Am. Chem. Soc. 2012, 134, 3895−3902

Table 1. Kinetic Parameters of Each Substrate for Xyl4

substrate	K_M (μM)	k_{cat} (s^{-1})	k_{cat}/K_M ($mM^{-1}\cdot s^{-1}$)
5	$(1.7 \pm 0.1) \times 10^3$	1.9	1.1
6	$(7.1 \pm 0.2) \times 10^2$	2.1	3.0
7	3.8 ± 0.1	0.89	2.3×10^2
12	nd	n.d.	n.d.

trisaccharide substrate **7**. Indeed, the k_{cat}/K_M value of trisaccharide **7** was some 210 and 80 times greater than those of the disaccharides **5** and **6**, respectively. This significant difference appears to be driven by tighter binding of the trisaccharide to Xyl4, as alluded to by the K_M values determined in these experiments. It is also possible that the lower K_M value could be a result of greater accumulation of the glycosyl–enzyme intermediate for the xylotrioside substrate. Equivalent enhanced accumulation of the intermediate was seen previously for the GH family 10 β-1,4-xylanase Cex[36] and was shown to result from an increase in the glycosylation rate constant due to addition of the extra sugar, with no effects on the deglycosylation rate constant. This explanation could also account for the considerably lower K_M values observed for the aryl glycoside substrates **5**–**7** relative to those reported for 1,3-xylotetraose and 1,3-xylopentaose.[17]

Thin layer chromatography and mass spectrometry revealed that the only carbohydrate product of the Xyl4-catalyzed hydrolysis of trisaccharide **7** (at ca. 50% completion) was 1,3-linked xylotriose, indicating that only the reducing-end glycosidic bond of this substrate is initially cleaved by the enzyme. It follows that Xyl4 possesses a −3 subsite that must be occupied for optimal activity, which is commensurate with the apparent *endo*-activity of Xyl4 on 1,3-xylan itself.[17] While the simple Michaelis–Menten kinetics observed for substrates **5** and **7** suggest that transglycosylation does not occur at a rate that is competitive with hydrolysis for this particular enzyme, it is interesting that the methylated disaccharide **6** was in fact a better substrate than the unmethylated disaccharide **5**. This difference appears to be driven by ground state binding interactions, as evidenced by differing K_M but similar k_{cat} values for the substrates. This phenomenon is typical of many *endo*-GHs and is likely a consequence of the fact that the natural polymeric substrates do not possess a free hydroxyl group at the position of methylation but instead have an "ether-like" oxygen capable only of accepting hydrogen bonds.[35] Finally, it should also be noted that Xyl4 had no detectable activity on 4-methylumbelliferyl β-D-xylopyranosyl-(1→4)-β-D-xyloside **12**, suggesting that a β-1,4-link between the −1 and −2 subsites of the enzyme is not tolerated.

Stereochemical Outcome of Xyl4-Catalyzed Hydrolysis. Since the 1,3-xylan substrate of Xyl4 is quite different from those of other enzymes from GH family 26, and given that at least one GH family has been shown to contain enzymes of opposing stereospecificities,[37] it was important to confirm that Xyl4 is indeed a retaining glycosidase, since this mechanistic feature is of particular relevance to the design of inhibitors. Accordingly, the hydrolysis of disaccharide substrate **5** was monitored directly by ^{1}H NMR (Figure S1 of the Supporting Information), revealing the initial, exclusive formation of the β-configured hemiacetal product. This confirmed that Xyl4 is indeed a retaining GH.

Competitive Inhibition. Having confirmed that Xyl4 utilizes a retaining mechanism and has a preference for β-1,3-linked trisaccharides over disaccharides, the design of competitive and mechanism-based inhibitors was considered. The classical mechanism of retaining GHs invokes transition states with considerable oxocarbenium ion character—placing partial positive charge on C-1 and O-5 of the pyranose ring. The potency of iminosugars as competitive inhibitors of GHs can be rationalized in terms of their mimicry of this partial positive charge developed at the transition state, although it is also reasonable to suggest that fortuitous Columbic interactions between a protonated iminosugar and the catalytic carboxylates of the enzyme contribute significantly to inhibitor potency. Potent competitive inhibitors of retaining 1,4-xylanases have been prepared by glycosylating (3*R*,4*R*)-3,4-dihydroxypiperidine, an iminosugar that is the D-xylose equivalent of the potent β-glucosidase inhibitor isofagomine, to produce 1,4-xylan-like oligosaccharides.[38,39] A similar approach to produce 1,3-xylan-like oligosaccharides **13** and **14** was expected to yield good 1,3-xylanase inhibitors.

Using established procedures, alcohol **15** was prepared and converted into pseudodisaccharide **13** (Scheme 3).[38,39]

Scheme 3. Synthesis of Competitive Inhibitors 13 and 14

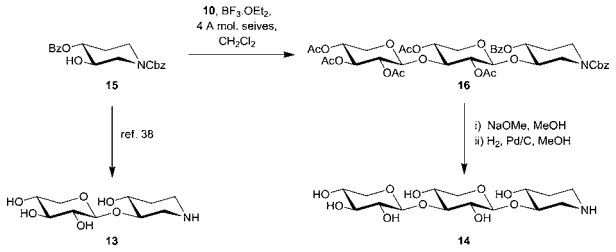

Disaccharide imidate **10** was used to glycosylate alcohol **15** to provide the pseudotrisaccharide **16**. This product was subjected to transesterification and hydrogenolysis to return the desired product **14**.

Iminosugars **13** and **14** were found to competitively inhibit Xyl4 with inhibition constants of 3.1 ± 0.3 mM and 2.0 ± 0.1 μM, respectively (Figure S2 of the Supporting Information). The almost 1000-fold difference between these K_i values illustrates once again that the −3 subsite of Xyl4 makes a significant contribution to ligand recognition. A comparison of the K_i values of the inhibitors to the K_M values determined for the corresponding disaccharide **5** (1.7 ± 0.1 mM) and trisaccharide **7** (3.8 ± 0.1 μM) substrates indicates that these iminosugars are in fact relatively poor inhibitors of Xyl4. A similar phenomenon has been observed for analogous β-1,4-linked iminosugars with a GH family 11 1,4-xylanase from *Bacillus circulans* (Bcx).[38] In that case it was proposed that the poor inhibition of Bcx was the result of the iminosugars failing to mimic the conformation of the pyranose ring in the −1 subsite at the enzyme's transition state. This was a reasonable explanation, since Bcx utilizes a somewhat unorthodox $^5S_1 \rightarrow {}^{2,5}B \rightarrow {}^2S_O$ conformational itinerary,[24,40] which is very different from the $^1S_3 \rightarrow {}^4H_3 \rightarrow {}^4C_1$ itinerary of the GH family 10 xylanases that were potently inhibited by the same iminosugars.[41] This raises the interesting possibility that iminosugars **13** and **14** are poor inhibitors of Xyl4 because this enzyme utilizes a similar conformational itinerary to that of the 1,4-xylanases of GH family 11. If so, then GH family 26 would be the first GH family demonstrated to utilize at least three different conformational itineraries to effect catalysis. This intriguing idea provided an added incentive to develop a novel mechanism-based inhibitor of 1,3-xylanases that functions via

dx.doi.org/10.1021/ja211836t | J. Am. Chem. Soc. 2012, 134, 3895–3902

the accumulation of the glycosyl−enzyme intermediate. Not only could such a molecule be a more effective inhibitor of these enzymes, but it would also provide a way to address the question of the enzyme's conformational itinerary using X-ray diffraction methods.

Mechanism-Based Inhibition by Accumulation of a Covalent Intermediate. Activated 2-deoxy-2-fluoroglycosides are frequently used as mechanism-based inhibitors of retaining glycosidases, with potent inhibition being achieved through the accumulation of a covalent glycosyl−enzyme intermediate.[42] When the hydroxyl group at C-2 of a glycoside is replaced with fluorine, the oxocarbenium ion-like transition states for formation and turnover of the glycosyl−enzyme intermediate are destabilized both through inductive effects and through the loss of transition state-stabilizing interactions between that hydroxyl group and the enzyme. Installation of a good nucleofuge at C-1 of the fluorosugar inhibitor accelerates the first step, enabling formation of the glycosyl−enzyme intermediate. However, hydrolysis of this glycosyl−enzyme intermediate remains slow, so the intermediate accumulates and enzyme activity is lost. Because Xyl4 has a strong preference for trisaccharide substrates, synthetic efforts were directed at preparing an activated 2-deoxy-2-fluoro trisaccharide to inhibit 1,3-xylanases. To this end, the alcohol **17** was prepared from D-xylose according to established methods[27] and then glycosylated using the disaccharide imidate **10** to provide the trisaccharide **18**. This product was deprotected by the action of methanolic hydrogen chloride to provide trisaccharide **19** (Scheme 4).

Scheme 4. Synthesis of a Mechanism-Based Inhibitor 19

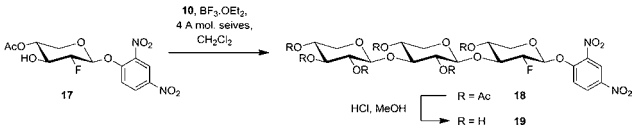

The trisaccharide fluorosugar **19** rapidly inactivated Xyl4 in a time-dependent manner with a second-order rate constant (k_i/K_i) of 129 ± 1 $mM^{-1}\cdot s^{-1}$ at 37 °C; the rapidity of the reaction precluded an estimation of the individual parameters k_i and K_i (Figure 1). Indeed, this is one of the most efficient mechanism-based inactivators of any glycosidase to date. To provide some context, inactivations of 1,4-xylanases from GH family 10 and 11 with analogous activated fluorosugars are reported to proceed with k_i/K_i rate constants in the range 0.007−0.3 $mM^{-1}\cdot s^{-1}$.[27,29] As a consequence, complete inactivation of Xyl4 can be achieved within an hour at low nanomolar concentrations of **19**. Proof that the inactivation by **19** is indeed active site-directed was provided by the protection against inactivation afforded by competitive inhibitor **14** (Figure S3). A 2.0 μM concentration of **14** (K_i = 2.0 ± 0.1 μM) decreased the observed rate of inactivation by 60 nM **19** from 8.4 ± 0.4 × 10^{-3} s^{-1} to 4.3 ± 0.1 × 10^{-3} s^{-1}.

The 2-fluoroxylotriosyl-enzyme species was shown to be catalytically competent, since it reactivated by spontaneous hydrolysis. However, hydrolytic turnover was determined to be relatively slow, with a rate constant for hydrolysis of just 1.1 ± 0.1 × 10^{-5} s^{-1}, corresponding to a half-life of 17.5 h (Table 2, Figure S4). Consistent with the catalytic relevance of the trapped intermediate, reactivation was accelerated by trans-glycosylation onto various D-xyloside acceptors. However, again this reactivation was not fast: incubation with a 20 mM

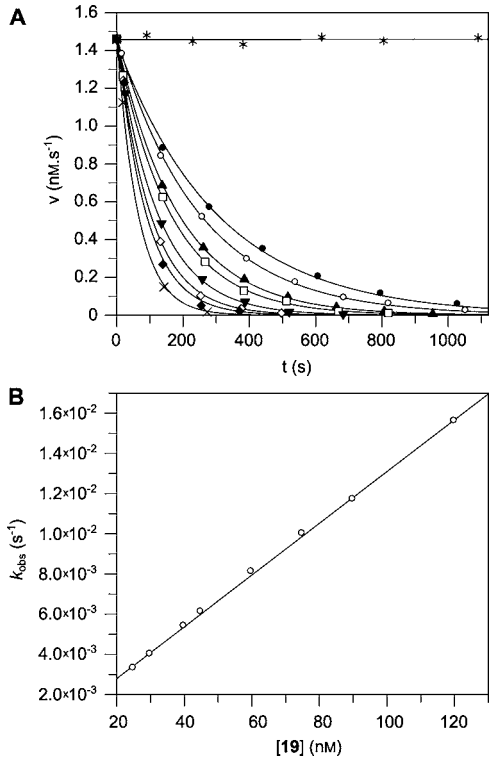

Figure 1. Time dependent inactivation of Xyl4 by **19**. (A) Plot of Xyl4 activity with respect to time when incubated at 37 °C with **19** at the following concentrations: 0 nM (∗); 25 nM (●); 30 nM (○); 40 nM (▲); 45 nM (□); 60 nM (▼); 75 nM (◇); 90 nM (◆); and 120 nM (×). Each curve represents a nonlinear fit of each data set to a single exponential decay equation, except for the data set collected in the absence of **19**, which was fit to a linear regression model. (B) Plot of the observed rate constants as a function of inactivator **19** concentration. This data was best fit by a linear regression model, the gradient of which provides an estimate of the second-order rate constant of inactivation k_i/K_i.

concentration of the 1,3-xylobioside **20**, a molecule very similar to the reducing end fragment of a natural substrate, increased the rate of reactivation by a factor of just 3. Very little, if any, increase in the rate of reactivation was observed for 1,4-xylobioside **21**[43] or xyloside **22**.[39] The greater rate of reactivation observed in the presence of 1,3-xylobioside **20** than either 1,4-xylobioside **21** or xyloside **22** alludes to the presence of a +2 subsite and a preference of the +1/+2 subsites for β-1,3-linked oligosaccharides. This observation is once again commensurate with the enzyme's *endo*-activity on natural 1,3-xylan.

Identification of the Catalytic Nucleophile. Sequence alignment of Xyl4 with the mannanases of GH family 26 suggests that the catalytic nucleophile should be E234. Inactivator **19** provided a convenient tool to obtain direct empirical evidence to confirm this assignment. Thus, samples of Xyl4 were incubated with or without inactivator **19** for several hours, thermally denatured, and digested with pepsin. Both peptidic digests (inactivated and a control) were analyzed by reverse-phase high performance liquid chromatography mass spectrometry (HPLC-MS), which enabled the identification of two glycosylated peptides that are unique to the labeled sample (m/z = 960.0 and 1016.6, z = 2) and their unlabeled counterparts (m/z = 761.0 and 817.5, z = 2) in the control sample. These peptides were sequenced by tandem mass

dx.doi.org/10.1021/ja211836t | J. Am. Chem. Soc. 2012, 134, 3895−3902

Table 2. Reactivation of 2-Fluoroxylotriosyl-Xyl4 through Hydrolysis and Transglycosylation

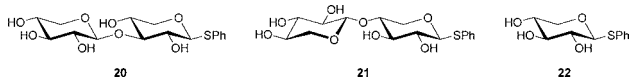

20 21 22

acceptor (20 mM)	reactivation rate constant, k (s^{-1})	half-life for reactivation, $t_{1/2}$ (h)
	$(1.1 \pm 0.1) \times 10^{-5}$	17.5
20	$(3.4 \pm 0.2) \times 10^{-5}$	5.7
21	$(1.4 \pm 0.1) \times 10^{-5}$	13.8
22	$(1.3 \pm 0.1) \times 10^{-5}$	14.8

spectrometry (MS-MS), which revealed that the putative nucleophile E234 was indeed glycosylated (Figure 2).

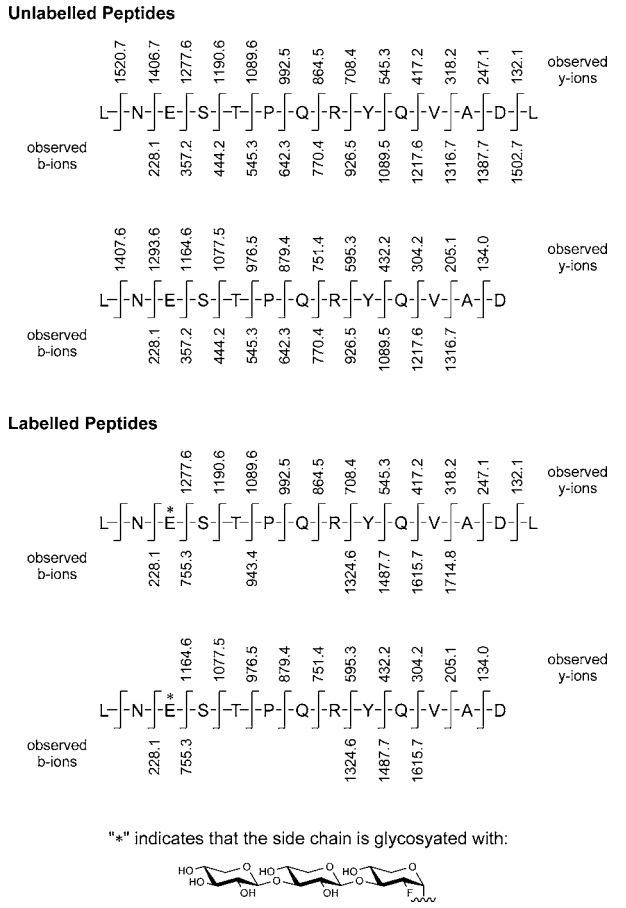

Figure 2. Identification of the catalytic nucleophile of Xyl4 by mass spectrometry using **19**.

Structure of the Trapped Glycosyl–Enzyme Intermediate. To address the question of what conformational itinerary the 1,3-xylanases might use, the structure of the catalytic domain of Xyl4 after inactivation with **19** was determined using X-ray diffraction methods to a resolution of 1.2 Å. Well-defined electron density was observed for the complete ligand, clearly revealing a covalent bond between C-1 of the proximal 2-deoxy-2-fluoro-D-xylose unit and the side chain carboxylate of E234 in the −1 subsite (Figure 3A). The interactions of the pyranose units in the −1 and −2 subsites with Xyl4 are typical for a glycosidase (Figure 3B). The D-xylose unit in the −3 subsite, which is very important for enzyme activity, makes few direct interactions with the protein but is an integral part of a large hydrogen-bonding network that facilitates many water-mediated interactions with Xyl4. Clearly

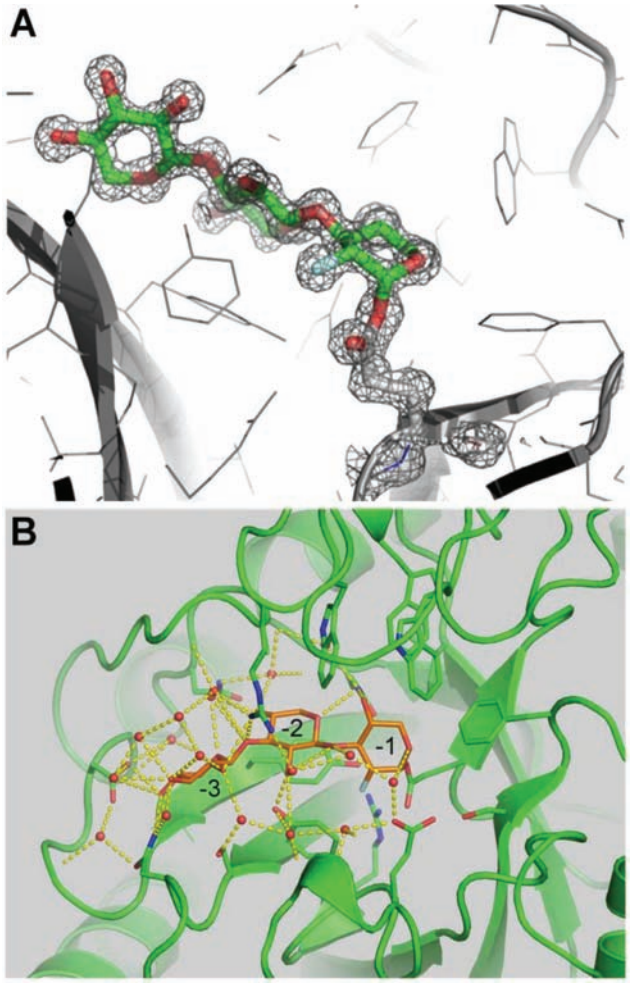

Figure 3. Covalent glycosyl–enzyme intermediate obtained by inactivation of Xyl4 with 19. (A) The electron density shown is a $2F_{obs} - F_{calcd}$ map contoured at 1σ. (B) Illustration of the interactions made by the covalently bound trisaccharide (orange) with Xyl4 (green) and the surrounding ordered water molecules.

these water-mediated interactions are important for catalysis. The covalently bound 2-deoxy-2-fluoroxylopyranosyl moiety adopts a $^4C_1$ conformation, which indicates that the 1,3-xylanases do not operate via an intermediate with the $^{2,5}B$ conformation, as had been thought probable, but rather utilize the $^1S_3 \rightarrow {}^4H_3 \rightarrow {}^4C_1$ conformational itinerary. In this regard, they are therefore similar to the lichenases of GH family 26[26] and the 1,4-xylanases of GH family 10.[44] This means that conformational considerations cannot explain the poor inhibitory activity of the iminosugars **13** and **14**. Further kinetic, thermodynamic, and structural investigations will be necessary to address that question.

dx.doi.org/10.1021/ja211836t | J. Am. Chem. Soc. 2012, 134, 3895–3902

CONCLUSION

A collection of 1,3-xylanase substrates has been synthesized and validated on the 1,3-xylanase from *Vibrio* sp. strain AX-4. This enzyme was confirmed to be a retaining glycosidase and demonstrated to have a marked preference for trisaccharide substrates, which is commensurate with its reported *endo*-activity. Two isofagomine-like oligosaccharides were prepared and shown to be relatively poor inhibitors of the xylanase, with K_i values that are comparable to the K_M value of the analogous substrates. A 2,4-dinitrophenyl 2-deoxy-2-fluoroxylotrioside was also synthesized and found to be an excellent mechanism-based inhibitor of the xylanase that functions through the formation of a stable, but catalytically competent, glycosyl−enzyme intermediate. Using this inactivator, the catalytic nucleophile of the enzyme was identified unequivocally by liquid chromatography−mass spectrometric analysis of proteolytic digests, and through reactivation experiments, evidence was obtained that the +1/+2 subsites have a preference for β-1,3-linked xylooligosaccharides. Finally, X-ray diffraction methods were used to determine the structure of the inactivated xylanase, providing evidence that these enzymes likely utilize a $^1S_3 \rightarrow {}^4H_3 \rightarrow {}^4C_1$ conformational itinerary to effect catalysis, much like the lichenases that also reside in GH family 26. Together, the compounds prepared and tested here represent an excellent set of molecular tools that set the stage for more detailed kinetic and structural studies of this biotechnologically relevant class of enzymes.

EXPERIMENTAL SECTION

General Materials and Methods. All chemicals were obtained from the Sigma-Aldrich Chemical Co. (USA) or SynChem Inc. (USA) and were of reagent grade. Thin layer chromatography (tlc) was performed on Merck silica gel 60 F_{254} plates. Flash chromatography was performed with Merck silica gel 60 (230−400 mesh). ^{1}H and ^{13}C NMR spectra (referenced using the residual solvent peak or an internal MeOH standard in the case of ^{13}C for D_2O) were recorded on a Bruker AV-300 or AV-400 instrument. High-resolution mass spectra of all compounds were obtained in the mass spectrometry laboratory of the Chemistry Department at U.B.C.

Enzymology. Xyl4 was recombinantly expressed in *E. coli*, as described previously.[17] All experiments with Xyl4 were conducted at 37 °C using a NaH_2PO_4/Na_2HPO_4 buffer (50 mM, pH 7.5) containing 150 mM NaCl and 0.1% w/v bovine serum albumin (BSA) unless otherwise stated. Reactions were initiated by the addition of Xyl4 to a solution of substrate (and inhibitor) in the aforementioned buffer. The increase in absorbance (400 nm) or fluorescence (λ_{ex} = 380 nm, λ_{em} = 500 nm) of the reaction mixture over time gave the initial reaction rate. Initial rates were constant over the 3 min for which each reaction was monitored. Michaelis parameters (v_{max} and K_m) for substrates **5**−**7** with Xyl4 were determined by a nonlinear fit of the initial rates at different substrate concentrations to the Michaelis−Menten equation using the GraFit 5.0.13 program. To determine the K_i value of inhibitors **13** and **14** for Xyl4, a series of initial reaction rates were measured at four concentrations of substrate **5** and a range of inhibitor concentrations (typically bracketing the K_i value ultimately determined such that $0.2K_i$ < [inhibitor] < $5K_i$). These data were fit to a competitive inhibition model using nonlinear regression analysis, as performed by the GraFit 5.0.13 program, to provide the K_i value. Dixon and Lineweaver−Burke plots of each data set validated the use of a competitive inhibition model. To determine the second-order rate constant of inactivation (k_i/K_i) of Xyl4 by **19**, pseudo-first-order rate constants, where $k_{obs} = k_i[\mathbf{19}]/(K_i + [\mathbf{19}])$, were measured for the decay in 1,3-xylanase activity at various concentrations of **19** (25, 30, 40, 45, 60, 75, 90, and 120 nM, as well as a control of 0 nM). Inactivation reactions were initiated by the addition of Xyl4 to a solution of **19** in buffer and incubated at 37 °C. Aliquots of the reactions were removed at appropriate time points and diluted into cuvettes containing substrate **7** in buffer. The initial rates of these reactions were determined as described above and represent a measure of the residual xylanase activity in the inactivation mixture at that time point. The initial rates obtained at each time point for a given concentration of **19** were fit to a single exponential decay equation using nonlinear regression with the program Grafit 5.0.13 to provide the pseudo-first-order rate constant of inactivation at that concentration of **19**. A plot of these pseudo-first-order rate constants against the concentration of **19** (Figure 1) suggested that the greatest concentration of **19** used in these experiments (120 nM) was in fact much less than K_i, and so the data was fit to a linear regression model with $k_{obs} \approx k_i[\mathbf{19}]/K_i$, to provide the second-order rate constant (k_i/K_i) of inactivation. To determine the rate of hydrolysis of the glycosyl−enzyme intermediate generated by the inactivation of Xyl4 by **19**, or its rate of transglycosylation onto acceptors **20**−**22** (at a concentration of 20 mM), a sample of Xyl4 was first incubated with **19** (90 nM) in buffer at 37 °C for 2 h. This sample was concentrated to 2% of its original volume at 4 °C using a centrifugal filter tube (Millipore, Biomax 30K NMWL membrane) and diluted to its original volume with a NaH_2PO_4/Na_2HPO_4 buffer (50 mM, pH 7.5) containing 150 mM NaCl. This process was repeated three times, and then samples were diluted further into the same buffer with or without one of the acceptors **20**−**22** (final concentration 20 mM). The mixtures were incubated at 37 °C, and aliquots were removed at appropriate time points and diluted into cuvettes containing substrate **7** in buffer. The initial rates of these reactions were determined as described above and represent a measure of the residual xylanase activity in the reactivation mixture at that time point. The initial rate data obtained for each reactivation experiment were modeled to first-order reaction kinetics using nonlinear regression by the program Grafit 5.0.13 to provide a pseudo-first-order rate constant of reactivation.

Identification of the Catalytic Nucelophile of Xyl4 by Mass Spectrometry. Xyl4 (1.0 mg·mL^{-1}) was inactivated by **19** (0.1 mM) as described above, except in the absence of BSA. This inactivated sample and a control sample of untreated Xyl4 (1.0 mg·mL^{-1}) were concentrated to 2% of their original volume at 4 °C using a centrifugal filter tube (Millipore, Biomax 30K NMWL membrane) and diluted with NaH_2PO_4/Na_2HPO_4 buffer (50 mM, pH 2.0) to their original volume. These samples were thermally denatured (90 °C, 2 min), cooled to 25 °C, and subjected to proteolysis by the addition of pepsin (final concentration 0.1 mg·mL^{-1}). After 3 h at 25 °C, digestion was halted by freezing the samples at −80 °C. The proteolysis products were analyzed by HPLC-MS immediately after thawing. Peptides were separated by reverse phase HPLC interfaced directly with a mass spectrometer. Mass spectra were obtained with a triple quadrupole mass spectrometer equipped with an ionspray ion source. Each proteolytic digest was loaded onto a C-18 column equilibrated with 0.05% CF_3CO_2H and 2.0% MeCN in H_2O (v/v, solvent A). The peptides were eluted with a gradient of 0−60% solvent B [0.045% CF_3CO_2H and 80% MeCN in H_2O (v/v)] over 60 min, followed by 100% solvent B for 2 min. Solvents were pumped at a constant flow rate of 50 μL·min^{-1}. Spectra were obtained in the single-quadrupole scan mode (HPLC-MS) or in the tandem MS-product scan mode (MS-MS). In the HPLC-MS mode, the quadrupole mass analyzer was scanned over a mass to charge ratio (m/z) range of 300−2200 amu with a step size of 0.5 amu and a dwell-time of 1.5 ms per step. The ion source voltage was set at 5.5 kV, and the orifice energy was 45 V. In the MS-MS mode, the spectra were obtained by selectively introducing the precursor peptide with the m/z value of interest from the first quadrupole (Q1) into the collision cell (Q2) and observing the fragment ions in the third quadrupole (Q3). The Q3 scan range was 50−1900 atomic mass units with the same step size and dwell time as above.

X-ray Structure Analysis. The recombinant Xyl4 catalytic module (rXYL4-CM) was prepared and crystallized as described previously.[45] Crystals were transferred into the reservoir solution with 110% precipitant containing 10 mM **19** and then incubated for 2 weeks. X-ray diffraction data up to 1.2 Å were collected using the synchrotron

dx.doi.org/10.1021/ja211836t | J. Am. Chem. Soc. 2012, 134, 3895−3902

radiation source at the beamline BL-17A of the Photon Factory (Ibaraki, Japan). The data were processed using HKL2000.[46] The structure of rXYL4-CM in complex with β-D-xylopyranosyl-(1→3)-β-D-xylopyranosyl-(1→3)-2-deoxy-2-fluoro-α-D-xylopyranosyl was determined by molecular replacement using the native rXYL4-CM structure (Protein Data Bank code 2DDX) with the program Molrep.[47] Manual model fitting and the structure refinement were performed with the programs Coot[48] and Refmac5.[49]

■ ASSOCIATED CONTENT

Supporting Information

Experimental information for the synthesis of novel compounds, demonstration of the retaining mechanism of Xyl4 using ^{1}H NMR spectroscopy, Dixon plots for inhibition of Xyl4 by **13** and **14**, reactivation experiments on inactivated Xyl4, and ^{1}H and ^{13}C NMR data for all novel compounds. This material is available free of charge via the Internet at http://pubs.acs.org.

■ AUTHOR INFORMATION

Corresponding Author

withers@chem.ubc.ca

Present Address

[‖]Institute for Biomedical Aging Research, Austrian Academy of Sciences, Innsbruck A-6020, Austria.

Notes

The authors declare no competing financial interest.

■ ACKNOWLEDGMENTS

E.D.G.B thanks the Canadian Institutes of Health Research for a postdoctoral fellowship. S.R. thanks the Austrian Science Fund for an Erwin Schrödinger Fellowship. S.G.W. acknowledges support from the Natural Sciences and Engineering Research Council of Canada, the Canada Research Chairs Program, the Canadian Foundation for Innovation, and the B.C. Knowledge Development Fund. We thank Shouming He of the Proteomics Core Facility at UBC for mass spectrometric analyses.

■ REFERENCES

(1) Correns, C. *Ber. Dtsch. Bot. Ges.* **1894**, *12*, 355.
(2) Nicolai, E.; Preston, R. D. *Proc. R. Soc. B* **1952**, *140*, 244−274.
(3) Veluraja, K.; Atkins, E. D. T. *Carbohydr. Polym.* **1987**, *7*, 133−141.
(4) Atkins, E. D. T.; Parker, K. D.; Preston, R. D. *Proc. R. Soc. B* **1969**, *173*, 209−221.
(5) Frei, E.; Preston, R. D. *Proc. R. Soc. London B* **1964**, *160*, 293−313.
(6) MacArtain, P.; Gill, C. I. R.; Brooks, M.; Campbell, R.; Rowland, I. R. *Nutr. Rev.* **2007**, *65*, 535−543.
(7) Nguyen, V. T.; Ueng, J.-P.; Tsai, G.-J. *J. Food. Sci.* **2011**, *76*, C950−C958.
(8) Meusnier, I.; Olsen, J. L.; Stam, W. T.; Destombe, C.; Valero, M. *Mol. Ecol.* **2001**, *10*, 931−946.
(9) Araki, T.; Hayakawa, M.; Tamaru, Y.; Yoshimatu, K.; Morishita, T. *J. Phycol.* **1994**, *30*, 1040−1046.
(10) Umemoto, Y.; Shibata, T.; Araki, T. *Mar. Biotechnol.* **2012**, *14*, 10−20.
(11) Iriki, Y.; Suzuki, T.; Nisizawa, K.; Miwa, T. *Nature* **1960**, *187*, 82−83.
(12) Chen, W. P.; Matsuo, M.; Yasui, T. *Agric. Biol. Chem.* **1986**, *50*, 1183−1194.
(13) Araki, T.; Inoue, N.; Morishita, T. *J. Gen. Appl. Microbiol.* **1998**, *44*, 269−274.
(14) Araki, T.; Tani, S.; Maeda, K.; Hashikawa, S.; Nakagawa, H.; Morishita, T. *Biosci. Biotechnol. Biochem.* **1999**, *63*, 2017−2019.
(15) Yamaura, I.; Matsumoto, T.; Funatsu, M.; Mukai, E. *Agric. Biol. Chem.* **1990**, *54*, 921−926.
(16) Araki, T.; Hashikawa, S.; Morishita, T. *Appl. Environ. Microbiol.* **2000**, *66*, 1741−1743.
(17) Kiyohara, M.; Sakaguchi, K.; Yamaguchi, K.; Araki, T.; Nakamura, T.; Ito, M. *Biochem. J.* **2005**, *388*, 949−957.
(18) Okazaki, F.; Tamaru, Y.; Hashikawa, S.; Li, Y.-T.; Araki, T. *J. Bacteriol.* **2002**, *184*, 2399−2403.
(19) Cantarel, B. L.; Coutinho, P. M.; Rancurel, C.; Bernard, T.; Lombard, V.; Henrissat, B. *Nucleic Acids Res.* **2009**, *37*, D233−D238.
(20) Hashimoto, H.; Tamai, Y.; Okazaki, F.; Tamaru, Y.; Shimizu, T.; Araki, T.; Sato, M. *FEBS Lett.* **2005**, *579*, 4324−4328.
(21) Kiyohara, M.; Sakaguchi, K.; Yamaguchi, K.; Araki, T.; Ito, M. *J. Biochem.* **2009**, *146*, 633−641.
(22) Bolam, D. N.; Hughes, N.; Virden, R.; Lakey, J. H.; Hazlewood, G. P.; Henrissat, B.; Braithwaite, K. L.; Gilbert, H. J. *Biochemistry* **1996**, *35*, 16195−16204.
(23) Taylor, E. J.; Goyal, A.; Guerreiro, C. I. P. D.; Prates, J. A. M.; Money, V. A.; Ferry, N.; Morland, C.; Planas, A.; Macdonald, J. A.; Stick, R. V.; Gilbert, H. J.; Fontes, C. M. G. A.; Davies, G. J. *J. Biol. Chem.* **2005**, *280*, 32761−32767.
(24) Davies, G. J.; Ducros, V. M.-A.; Varrot, A.; Zechel, D. L. *Biochem. Soc. Trans.* **2003**, *31*, 523−527.
(25) Ducros, V. M.-A.; Zechel, D. L.; Murshudov, G. N.; Gilbert, H. J.; Szabó, L.; Stoll, D.; Withers, S. G.; Davies, G. J. *Angew. Chem., Int. Ed.* **2002**, *41*, 2824−2827.
(26) Money, V. A.; Smith, N. L.; Scaffidi, A.; Stick, R. V.; Gilbert, H. J.; Davies, G. J. *Angew. Chem., Int. Ed.* **2006**, *45*, 5136−5140.
(27) Ziser, L.; Setyawati, I.; Withers, S. G. *Carbohydr. Res.* **1995**, *274*, 137−153.
(28) McIntosh, L. P.; Hand, G.; Johnson, P. E.; Joshi, M. D.; Körner, M.; Plesniak, L. A.; Ziser, L.; Wakarchuk, W. W.; Withers, S. G. *Biochemistry* **1996**, *35*, 9958−9966.
(29) Miao, S.; Ziser, L.; Aebersold, R.; Withers, S. G. *Biochemistry* **1994**, *33*, 7027−7032.
(30) Notenboom, V.; Williams, S. J.; Hoos, R.; Withers, S. G.; Rose, D. R. *Biochemistry* **2000**, *39*, 11553−11563.
(31) Wicki, J.; Schloegl, J.; Tarling, C. A.; Withers, S. G. *Biochemistry* **2007**, *46*, 6996−7005.
(32) Ludwiczek, M. L.; Heller, M.; Kantner, T.; McIntosh, L. P. *J. Mol. Biol.* **2007**, *373*, 337−354.
(33) Mori, M.; Ito, Y.; Ogawa, T. *Carbohydr. Res.* **1990**, *195*, 199−224.
(34) Utille, J.-P.; Gagnaire, D. *Carbohydr. Res.* **1982**, *106*, 43−57.
(35) Damager, I.; Numao, S.; Chen, H. M.; Brayer, G. D.; Withers, S. G. *Carbohydr. Res.* **2004**, *339*, 1727−1737.
(36) Tull, D.; Withers, S. G. *Biochemistry* **1994**, *33*, 6363−6370.
(37) Gloster, T. M.; Turkenburg, J. P.; Potts, J. R.; Henrissat, B.; Davies, G. *J. Chem. Biol.* **2008**, *15*, 1058−1067.
(38) Williams, S. J.; Hoos, R.; Withers, S. G. *J. Am. Chem. Soc.* **2000**, *122*, 2223−2235.
(39) Goddard-Borger, E. D.; Fiege, B.; Kwan, E. M.; Withers, S. G. *ChemBioChem* **2011**, *12*, 1703−1711.
(40) Sidhu, G.; Withers, S. G.; Nguyen, N. T.; McIntosh, L. P.; Ziser, L.; Brayer, G. D. *Biochemistry* **1999**, *38*, 5346−5354.
(41) White, A.; Tull, D.; Johns, K.; Withers, S. G.; Rose, D. R. *Nat. Struct. Biol.* **1996**, *3*, 149−154.
(42) Withers, S. G.; Street, L. P.; Bird, P.; Dolphin, D. H. *J. Am. Chem. Soc.* **1987**, *109*, 7530−7531.
(43) López, R.; Fernádez-Mayoralas, A. *J. Org. Chem.* **1994**, *59*, 737−745.
(44) Notenboom, V.; Birsan, C.; Warren, R. A. J.; Withers, S. G.; Rose, D. R. *Biochemistry* **1998**, *37*, 4751−4758.
(45) Sakaguchi, K.; Kiyohara, M.; Watanabe, N.; Yamaguchi, K.; Ito, M.; Kawamura, T.; Tanaka, I. *Acta Crystallogr., D: Biol. Crystallogr.* **2004**, *60*, 1470−1472.
(46) Otwinowski, Z.; Minor, W. *Methods Enzymol.* **1997**, *276*, 307−326.

(47) Vagin, A.; Teplyakov, A. *Acta Crystallogr., D: Biol. Crystallogr.* **2000**, *56*, 1622−1624.
(48) Emslcy, P.; Cowtan, K. *Acta Crystallogr., D: Biol. Crystallogr.* **2004**, *60*, 2126−2132.
(49) Murshudov, G. N.; Vagin, A. A.; Dodson, E. J. *Acta Crystallogr., D: Biol. Crystallogr.* **1997**, *53*, 240−255.